

Delaying transition to turbulence in channel flow: revisiting the stability of shear-thinning fluids

C. NOUAR¹, A. BOTTARO² AND J. P. BRANCHER¹

¹LEMETA, UMR 7563 (CNRS-INPL-UHP), 2 Avenue de la Fort de Haye,
BP 160 54504 Vandoeuvre Lès Nancy, France

²Università di Genova, Dipartimento di Ingegneria, delle Costruzioni, Ambiente e Territorio,
Via Montallegro 1, 16145 Genova, Italy

(Received 18 January 2007 and in revised form 21 July 2007)

A viscosity stratification is considered as a possible mean to postpone the onset of transition to turbulence in channel flow. As a prototype problem, we focus on the linear stability of shear-thinning fluids modelled by the Carreau rheological law. To assess whether there is stabilization and by how much, it is important both to account for a viscosity disturbance in the perturbation equations, and to employ an appropriate viscosity scale in the definition of the Reynolds number. Failure to do so can yield qualitatively and quantitatively incorrect conclusions. Results are obtained for both exponentially and algebraically growing disturbances, demonstrating that a viscous stratification is a viable approach to maintain laminarity.

1. Introduction

The problem of the control of fluid flow turbulence (often, but not always, to delay its occurrence or mitigate its effects) has many practical applications, from aeronautics to pipeline engineering. In an attempt to pursue effective control strategies, many different techniques have been proposed, comprehensively reviewed by Gad-el-Hak (2000). Among them, an approach to delay transition discussed many years ago by Craik (1969) has received much attention in recent years. It can be put in the category of the ‘stability modifiers’ and it consists of generating a small viscosity stratification in the fluid. If, for example, a laminar wall-bounded shear flow of a fluid system in which two layers of different viscosities are superimposed is considered, there may be a significant stabilizing effect. This is the case whenever the smaller viscosity fluid is close to the wall, provided that the viscous interface is positioned near the so-called critical layer, where the inviscid stability equation becomes singular (i.e. where the flow velocity matches locally the phase speed of the disturbance wave). This stabilization approach is attractive because it is *passive* (i.e. it does not require the input of energy into the system) and can be pursued very simply by introducing small quantities of a different fluid or of polymers in the channel, or by producing the required viscosity contrast with mild temperature or concentration gradients.

The beneficial effect of adding small concentrations of long-chain polymers to turbulent flows has been known for a long time (Lumley 1969; Metzner 1977; Bird, Armstrong & Hassager 1987). Friction drag is reduced drastically and the effect appears to be associated with the enhanced effective viscosity induced by the extensional thickening properties of polymeric solutions. Numerical observations

(Orlandi 1997; Sureshkumar Beris & Handler 1997; De Angelis Casciola & Piva 2002) show that turbulence-generating events in the buffer layer are inhibited by the presence of polymers: drag reduction is accompanied by a weakening of the streamwise vortices, a modification to fluctuating velocity characteristics, and an increase in the average spacing between the streaks within the buffer layer. A mechanistic explanation of the effects observed is emerging through the study of nonlinear recurrent states which mirror effects observed experimentally in buffer-layer turbulence of viscoelastic fluids (Stone *et al.* 2004; Li, Xi & Graham 2006).

Recent efforts aimed at assessing the effect of a stratification of viscosity examined the behaviour of small disturbances in laminar channel flows (Ranganathan & Govindarajan 2001, Govindarajan L'vov & Procaccia 2001, Govindarajan 2002, Govindarajan *et al.* 2003, Chikkadi Sameen & Govindarajan 2005). The results of these studies are summarized below:

(i) any spatial dependence of the viscosity μ in the critical layer, with μ decreasing towards the wall, is sufficient to considerably delay the onset of two-dimensional instability modes;

(ii) the effect is related to a reduced production of disturbance kinetic energy by interaction with the mean field; the energy dissipation responds less dramatically to changes in viscosity;

(iii) it is argued that in a turbulent configuration the energy budget could display a similar behaviour when the turbulence-production layer overlaps with the viscosity-stratified layer, with the same reduced-production mechanism active for each interacting mode;

(iv) the secondary three-dimensional instability modes are 'slaved' to the primary modes and are rapidly damped;†

(v) transient growth is relatively unaffected by viscosity gradients.

Some of the points above prompted the present investigation since their implications might have far-reaching consequences for flow control, and so we investigate further the linear stability issue, focusing on nonlinear, purely viscous fluids:

$$\boldsymbol{\tau} = \mu(\dot{\boldsymbol{\gamma}})\dot{\boldsymbol{\gamma}},$$

with $\boldsymbol{\tau}$ the deviatoric stress tensor and $\dot{\boldsymbol{\gamma}}$ the second invariant of the strain-rate tensor $\dot{\boldsymbol{\gamma}}$, defined by $\dot{\boldsymbol{\gamma}} = (\frac{1}{2}\dot{\boldsymbol{\gamma}} : \dot{\boldsymbol{\gamma}})^{1/2}$, with $\dot{\boldsymbol{\gamma}} = (\nabla\mathbf{u} + \nabla\mathbf{u}^T)$. On the one hand, understanding the phenomenon of transition initiated by the growth of infinitesimal perturbations is a necessary prerequisite to finding effective transition-delay strategies. On the other hand, it has been argued by Farrell & Ioannou (1998) that the mechanism responsible for the formation of coherent structures in near-wall turbulence obeys linear rules. It is thus possible that some of the findings reported here carry over to more complex situations.

We defer further analysis of the literature on viscously stratified flows to a later section, after having established the equations governing the problem. The paper is organized as follows: The linear stability equations are derived in §2. They differ from the equations reported previously, and a discussion on this difference is provided. In §3 the modal results are presented. The short-time behaviour of disturbances in the subcritical regime is discussed in §4; §5 contains a brief summary of the results obtained.

† The base flow considered in the secondary stability analysis consists of the steady profile plus the most unsteady travelling mode of the primary instability, with prescribed finite amplitude. The base flow is supposed frozen in time, which is admissible under the assumption of separation of scales.

2. Set-up of the problem

The motion of an incompressible, shear-thinning fluid of negligible visco-elasticity in a channel bounded by two parallel plates located at $\hat{y} = \pm h$ is considered. The flow is driven by a constant gradient of pressure \hat{p} along the longitudinal direction \hat{x} . The dimensionless hydrodynamic equations are

$$\left(\frac{\partial}{\partial t} + \mathbf{u} \cdot \nabla \right) \mathbf{u} = -\nabla p + \nabla \cdot \boldsymbol{\tau}, \quad (2.1)$$

$$\nabla \cdot \mathbf{u} = 0. \quad (2.2)$$

Although the disturbance equations derived below are valid for any nonlinear purely viscous fluid, a rheological law must be chosen to model the shear-thinning behaviour of fluids such as colloidal suspensions, paints, dispersions or polymer solutions. Among the many possibilities (power-law, Ellis, Carreau–Yasuda, Cross etc) we have chosen the Carreau (1972) model for the following reasons:

(i) It has a sound theoretical basis, since it arises from Lodge's molecular network theory and has proven capable of modelling simultaneously the steady shear, complex viscosity, stress growth and stress relaxation functions;

(ii) It is frequently adopted to describe the rheological behaviour of pseudoplastic fluids and stability analysis data are available in the literature.

Unpublished results obtained by our group show that the conclusions to be reported below are qualitatively unaffected when the power-law constitutive model is used instead of the Carreau law.

The constitutive relation is thus

$$\boldsymbol{\tau} = \frac{1}{Re} \mu \dot{\boldsymbol{\gamma}} \quad \text{with} \quad \mu = \frac{\hat{\mu}_\infty}{\hat{\mu}_0} + \left[1 - \frac{\hat{\mu}_\infty}{\hat{\mu}_0} \right] [1 + (\lambda \dot{\boldsymbol{\gamma}})^2]^{(n-1)/2}; \quad (2.3)$$

the variables have been normalized with the half-channel thickness h , the centreline velocity U_c , the zero-shear-rate viscosity $\hat{\mu}_0$ and the dynamic pressure ρU_c^2 , with ρ the fluid density. The Reynolds number Re is defined as

$$Re = \frac{\rho U_c h}{\hat{\mu}_0}. \quad (2.4)$$

The infinite-shear-rate viscosity $\hat{\mu}_\infty$, which is generally associated with a breakdown of the fluid, is frequently significantly smaller (10^{-3} to 10^{-4} times) than $\hat{\mu}_0$, see Bird, Armstrong & Hassager (1987) and Tanner (2000). The ratio $\hat{\mu}_\infty/\hat{\mu}_0$ will be thus neglected in the following. The power-law index n represents the degree of shear thinning, the onset of which is function of the time constant of the material λ . Note that for $n=1$ or $\lambda=0$, the Carreau model describes the behaviour of a Newtonian fluid of viscosity $\hat{\mu}_0$ and if λ is very large, it reduces to the power-law model $\hat{\mu} = K \hat{\boldsymbol{\gamma}}^{n-1}$ with the consistency factor K defined by $K = \hat{\mu}_0 \hat{\lambda}^{n-1}$ ($\hat{\lambda}$ and $\hat{\boldsymbol{\gamma}}$ are dimensional quantities). An example of rheological data for polymer solutions is given by Bird *et al.* (1987). Typically, $0.2 \leq n < 1$ and $O(0.1) \leq \lambda < O(10^2)$.

2.1. Linear stability equations

We are interested in the stability of the steady unidirectional base flow $\mathbf{U}_b = U_b(y)\mathbf{e}_x$ satisfying equations (2.1–2.3), together with no-slip conditions at the rigid walls. Sample velocity distributions are plotted in figure 1 and it can be demonstrated that the profiles are ‘fuller’ for increasing values of the time constant of the fluid λ , for any fixed value of n . By analogy with previous results obtained by Fransson & Corbett (2003) for the asymptotic suction boundary layer and by Corbett & Bottaro (2000)

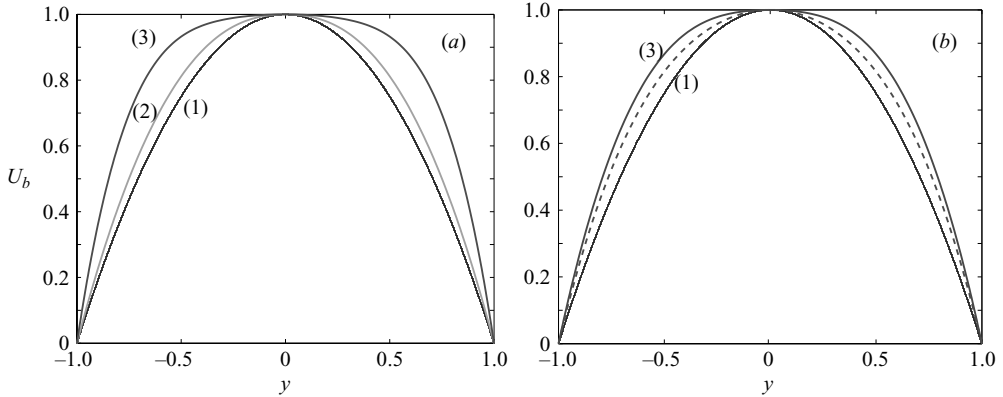


FIGURE 1. Velocity profiles. (a) Effect of n at $\lambda = 10$: (1) Newtonian; (2) $n = 0.7$ and (3) $n = 0.3$. (b) Effect of λ at $n = 0.5$: (1) Newtonian, (2, dashed-line) $\lambda = 1.5$ and (3) $\lambda = 10$.

for the boundary layer under conditions of favourable streamwise pressure gradient, it is not unreasonable to anticipate that the effect of shear thinning (increasing λ or decreasing n) is stabilizing, both from the point of view of the asymptotic behaviour of small disturbances and from that of the short-time transient behaviour. Unexpectedly, whereas the modal behaviour did indeed conform to expectations, the non-modal short-time results did not, leading Chikkadi *et al.* (2005) to “state firmly that a stratification of viscosity alone does not affect transient growth”. It will be argued below that such a conclusion is incorrect.

To characterize the stability of the flow, an infinitesimal perturbation ($\epsilon \mathbf{u}'$, $\epsilon p'$) is considered and the momentum equation is linearized around (\mathbf{U}_b, p_b) :

$$\frac{\partial \mathbf{u}'}{\partial t} = -(\mathbf{u}' \cdot \nabla) \mathbf{U}_b - (\mathbf{U}_b \cdot \nabla) \mathbf{u}' - \nabla p' + \nabla \cdot \boldsymbol{\tau}', \quad (2.5)$$

where $\boldsymbol{\tau}'$ is the shear stress perturbation given by $\boldsymbol{\tau}' = \mu(\mathbf{U}_b) \dot{\boldsymbol{\gamma}}(\mathbf{u}') + \mu' \dot{\boldsymbol{\gamma}}(\mathbf{U}_b)$ with μ' the viscosity perturbation:

$$\mu' = \dot{\gamma}_{ij}(\mathbf{u}') \frac{\partial \mu}{\partial \dot{\gamma}_{ij}}(\mathbf{U}_b). \quad (2.6)$$

Since the base flow is unidirectional, it can be shown straightforwardly that

$$\tau'_{ij} = \mu(\mathbf{U}_b) \dot{\gamma}_{ij}(\mathbf{u}') \quad \text{for } ij \neq xy, yx, \quad (2.7)$$

$$\tau'_{ij} = \mu_t(\mathbf{U}_b) \dot{\gamma}_{ij}(\mathbf{u}') \quad \text{for } ij = xy, yx, \quad (2.8)$$

where

$$\mu_t = \mu(\mathbf{U}_b) + \frac{d\mu}{d\dot{\gamma}_{xy}}(\mathbf{U}_b) \dot{\gamma}_{xy}(\mathbf{U}_b) \quad (2.9)$$

is termed the *tangent viscosity*. For a one-dimensional shear flow, with velocity $U_b(y)$ in the x -direction, the tangent viscosity is defined by $\mu_t = d\tau_{xy}/d\dot{\gamma}_{xy}$, as sketched in figure 2 for a given reference point (recall that the effective viscosity μ is experimentally defined as the ratio between τ_{xy} and $\dot{\gamma}_{xy}$ in a flow such as that considered here). For shear-thinning fluids we have $\mu_t < \mu$, whereas the opposite holds for shear-thickening fluids. It is important to observe that the fluctuating shear stress tensor $\boldsymbol{\tau}'$ is anisotropic, because of the presence of a viscosity perturbation. This is a

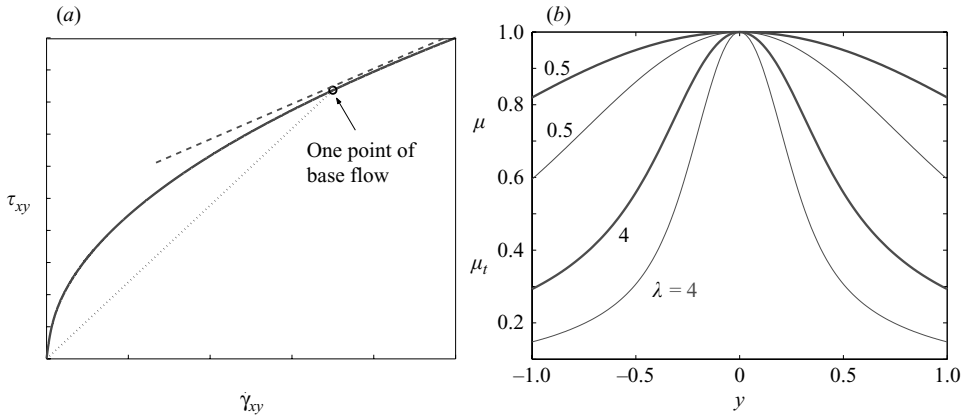


FIGURE 2. (a) Qualitative behavior of τ_{xy} versus $\dot{\gamma}_{xy}$ for a Carreau fluid. The slope of the dotted line is the so-called effective viscosity, the slope of the dashed line is the tangent viscosity. (b) Effective and tangent viscosity as functions of the wall-normal coordinate y , for $n=0.5$ and two values of λ . The thick line is the effective viscosity and the thin line is the tangent viscosity.

characteristic of nonlinear viscous fluids, with or without yield stress[†]. For instance, in the case of the Bingham–Poiseuille flow, τ'_{xy} is independent of the Bingham number, which is a dimensionless yield stress (Nouar *et al.* 2007). Since this appears to have been overlooked by some authors, a brief review of the literature is appropriate at this point.

2.2. Brief summary of research results on viscously stratified flows in channels

A stratification in viscosity can be obtained by considering different immiscible fluids in contact (in which case the viscosity presents a discontinuity), or when temperature and/or concentration gradients are involved (so that a diffusive interface of non-zero thickness is present), or in the case of non-Newtonian fluids. The case of two superposed immiscible fluids of constant (and different) viscosities was initially considered by Yih (1967) who focused on long waves and found an interfacial mode of instability at all Reynolds numbers. Hooper & Boyd (1983) later found that short waves can also be easily destabilized. The instability mechanism was studied by Hinch (1984) and Charru & Hinch (2000), who elucidated the roles of the layer thicknesses and of the viscosity ratio.

A smooth viscosity stratification can be obtained when μ depends on an intensive quantity obeying an advection–diffusion equation. The equations for two-dimensional stability modes, when μ is a linear functional of concentration or temperature alone, are given, for example, by Govindarajan (2002), under the assumption that the scalar diffusion coefficient is sufficiently small to allow the neglect of the thickening of the interface along x . Govindarajan’s equations correctly include the terms arising from a viscosity disturbance, so that a modified Orr–Sommerfeld equation is found, coupled to a linear scalar transport equation. The same equations have been employed by Wall & Wilson (1996), Ern, Charru & Luchini (2003) and, in the context of an exponential (rather than linear) viscosity–temperature relationship, by Pinarbasi & Liakopoulos (1995) and Sameen & Govindarajan (2007). Govindarajan (2002)

[†] For Newtonian fluids with a viscosity stratification induced, for instance, by temperature gradients $\boldsymbol{\tau}'$ remains isotropic.

indicates that her results are qualitatively different from those related to the interfacial stability of immiscible fluids; conversely, Ern *et al.* (2003) show that the stability of a diffused interface tends smoothly to that of the discontinuous case when the interface thickness tends to zero. In either case, the details of the stratification are crucial in determining the fate of small disturbances.

Other authors, e.g. Ranganathan & Govindarajan (2001), Govindarajan *et al.* (2001, 2003), Malik & Hooper (2005), do not include viscosity fluctuations in the linear stability equations. This can only be justified if an infinite scalar diffusion coefficient \mathcal{D} were considered for the perturbations; such an assumption is however untenable with the assumed steady viscosity stratification since, if $\mathcal{D} \rightarrow \infty$, the basic viscosity gradient cannot be maintained. In a similar vein, Zhang, Acrivos & Schaflinger (1992) performed a linear analysis for a flowing suspension of a *uniform* concentration of particles. As pointed out by Ern *et al.* (2003), the presence in related experiments of concentration gradients, and the existence of fluctuations in the concentration (and, as a consequence, in the fluid viscosity) could alter the conclusions.

The linear stability of non-Newtonian fluids to two-dimensional travelling wave modes in a plane channel with heat transfer has been studied by Pinarbasi & Ozalp (2001) for the case of inelastic liquids modelled by the Carreau constitutive equation. In this case, μ' was included in the analysis and considered a function of the shear rate only, dropping the (supposedly negligible) dependence on the temperature fluctuations. The same type of viscosity law was later adopted by Chikkadi *et al.* (2005), who also examined the case of two miscible fluids of equal densities and different viscosities. This latter analysis focused, in particular, on the problem of the transient growth of disturbances, a problem practically ignored until very recently in the literature of non-Newtonian fluids. In their paper Chikkadi *et al.* (2005) did not account for the anisotropic nature of the shear stress disturbance tensor.

A very recent paper by Saamen & Govindarajan (2007) addresses the effect of heating on the modal and non-modal stability of channel flow of a Newtonian fluid; the viscosity depends on temperature with an Arrhenius law. A decrease in viscosity towards the wall stabilizes normal modes, in line with previous findings; non-modal results are found to be significantly affected by an increase in Prandtl number and, surprisingly, optimal disturbances are found to be two-dimensional spanwise homogeneous. The paper employs a reference viscosity which is the value averaged across the normal-to-the-wall direction, as suggested by Wall & Wilson (1996).

The present contribution examines some of the assumptions that have appeared in the literature and the aim is at a rational assessment of the effect of a viscosity stratification on the modal and non-modal growth of disturbances. The question of which reference viscosity to adopt is also addressed.

2.3. Final equations

The disturbance field is assumed of the form $[\mathbf{u}', p'] = [\tilde{\mathbf{u}}(y, t), \tilde{p}(y, t)] \exp[i(\alpha x + \beta z)]$, with α and β the streamwise and spanwise wavenumbers, respectively. Equation (2.5) can be written in terms of the normal velocity \tilde{v} and the normal vorticity $\tilde{\eta} = i\beta\tilde{u} - i\alpha\tilde{w}$, so that the initial-value problem becomes

$$-i \begin{pmatrix} \mathcal{L} & \mathcal{C}_1 \\ \mathcal{C}_2 & \mathcal{S} \end{pmatrix} \begin{pmatrix} \tilde{v} \\ \tilde{\eta} \end{pmatrix} = \frac{\partial}{\partial t} \begin{pmatrix} \Delta \tilde{v} \\ \tilde{\eta} \end{pmatrix}, \quad (2.10)$$

where the operators \mathcal{L} , \mathcal{C}_1 , \mathcal{C}_2 and \mathcal{S} are defined as

$$\begin{aligned} \mathcal{L} = & \alpha[U_b \Delta - D^2 U_b] + \frac{i}{Re} [\mu \Delta^2 + 2D\mu D^3 + D^2 \mu D^2 - 2k^2 D\mu D + k^2 D^2 \mu] \\ & + i \frac{\alpha^2}{Re k^2} (D^2 + k^2) [(\mu_t - \mu)(D^2 + k^2)], \end{aligned} \quad (2.11)$$

$$\mathcal{C}_1 = -i \frac{\alpha \beta}{Re k^2} (D^2 + k^2) [(\mu_t - \mu)D], \quad (2.12)$$

$$\mathcal{C}_2 = \beta D U_b - i \frac{\alpha \beta}{Re k^2} D [(\mu_t - \mu)(D^2 + k^2)], \quad (2.13)$$

$$\mathcal{S} = \alpha U_b + \frac{i}{Re} \mu \Delta + \frac{i}{Re} D\mu D + \frac{i}{Re} \frac{\beta^2}{k^2} D [(\mu_t - \mu)D], \quad (2.14)$$

with $k^2 = \alpha^2 + \beta^2$; $D = d/dy$ and $\Delta = D^2 - k^2$.

A Chebyshev collocation method is used to solve (2.10) along with boundary conditions $\tilde{v} = D\tilde{v} = \tilde{\eta} = 0$ at $y \pm 1$. Standard techniques (described in Schmid & Henningson 2001 and references therein) are employed to compute eigenvalues, eigenmodes and transient energy growth. The convergence of the results has been verified and the code has been thoroughly tested by comparing both the modal and the non-modal results with those provided in Chikkadi *et al.* (2005).

3. Long-time behaviour of the disturbance: eigenvalue problem

When the long-time behaviour is sought, the disturbance mode can be assumed to vary exponentially with time, i.e. $[\tilde{v}, \tilde{\eta}](y, t) = [v, \eta](y; \alpha, \beta) e^{-i\omega t}$. The initial-value problem (2.10) is transformed into a generalized eigenvalue problem with the complex frequency ω as the eigenvalue. Since there is no equivalent of Squire's theorem for nonlinear viscous fluid, we have performed several tests for different values of $n \in [0.2, 1]$ and $\lambda \in [0, 20]$, as well as different wavenumbers α and $\beta \in [0, 5]$. The results indicate that the lowest critical Reynolds number is obtained for spanwise-homogeneous disturbances, i.e. $\beta = 0$. In hindsight, there are clues as to the validity of Squire's theorem: On the one hand, if μ' is artificially forced to zero, it can be shown easily that Squire's transformation holds (see, e.g., Drazin & Reid 1981), and that an equivalent two-dimensional problem can be defined. Secondly, when the viscosity perturbation is accounted for, its effect appears only through τ'_{xy} , present in the x - and y -perturbation equations and involving only axial and normal velocity disturbances. Finally, it is of significance that τ'_{xy} enters the tangent viscosity only, which is here smaller than μ .

The two-dimensional eigenvalue problem reduces to the solution of a Orr–Sommerfeld-like equation, $\mathcal{L}v = \omega \Delta v$. The even and odd v -modes decouple and may be considered separately, with boundary conditions on the channel centreline $y=0$ being $v = D^2 v = 0$ or $Dv = D^3 v = 0$ for odd and even symmetries, respectively. For Re greater than the critical value Re_c the even modes have a positive imaginary part, corresponding to a linearly unstable Tollmien–Schlichting wave. To compare our results with those in the literature, Re (based on the zero-shear-rate viscosity $\hat{\mu}_0$) is converted to \overline{Re} : the overbar defines a Reynolds number based on the viscosity averaged across the channel. This definition was suggested by Wall & Wilson (1996) for Newtonian fluids, to better represent the global decrease of μ when the channel walls were heated. Later, it was also adopted by Chikkadi *et al.* (2005) for Carreau fluids.

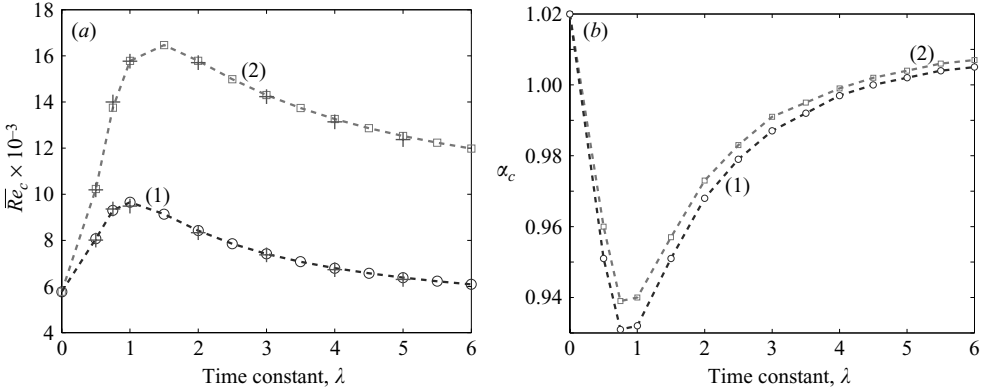


FIGURE 3. Variation of (a) the critical Reynolds number and (b) streamwise wavenumber with the time constant λ at $n=0.5$: line (1) corresponds to results including the viscosity perturbation and line (2) excluding the viscosity perturbation. The + signs correspond to unpublished data provided by Chikkadi & Govindarajan (2007).

The importance of the viscosity perturbation term is illustrated by figure 3(a) where the critical Reynolds number, \overline{Re}_c , is reported as a function of the time constant λ at $n=0.5$ and compared with the situation where μ' is artificially forced to zero. The results obtained for this last situation are in excellent agreement with those given by Chikkadi *et al.* (2005). The evolution of the corresponding streamwise wavenumber is also represented (figure 3b). In the range of the rheological parameters considered in figure 3, it is found that shear thinning stabilizes the flow, but the degree of stabilization is more modest when all terms are included in the equations, and the critical Reynolds number is about a factor of 2 smaller. The fact that including or excluding the viscosity perturbation gives rise to such large variations is, in itself, a significant result; V. Chikkadi & R. Govindarajan (2007, personal communication) indicate that such differences in critical Reynolds numbers are mildly attenuated when n increases from 0.5 to 0.7.

To interpret the effect of the viscosity disturbance, the modified Orr–Sommerfeld equation is multiplied by v^* , the complex conjugate of v , and integrated in y from the lower to the upper wall. Taking the real part of the result it is easy to obtain

$$\omega_i \langle |Dv|^2 + \alpha^2 |v|^2 \rangle = \alpha \langle DU_b(v_r Dv_i - v_i Dv_r) \rangle - \frac{1}{Re} \langle \mu(4\alpha^2 |Dv|^2 + |D^2v + \alpha^2 v|^2) \rangle + \frac{1}{Re} \langle (\mu - \mu_t) |D^2v + \alpha^2 v|^2 \rangle, \quad (3.1)$$

where $|v|^2 = v_r^2 + v_i^2$ and $\langle \cdot \rangle = \int_{-1}^1 (\cdot) dy$. The third term on the right-hand-side of (3.1) arises from the viscosity perturbation. It is a positive-definite term for shear-thinning fluids ($\mu_t < \mu$) which has the consequence that viscous dissipation is reduced compared to the case with $\mu' = 0$. Hence, the onset of instability is found earlier than in the $\mu' = 0$ case. When an infinitesimal perturbation is imposed on the basic flow, the shear stress and the shear rate are disturbed by $\delta\tau_{xy}$ and $\delta\dot{\gamma}_{xy}$, so that the disturbance field ‘will feel’ the (smaller) tangent viscosity $\mu_t = \delta\tau_{xy}/\delta\dot{\gamma}_{xy}$, sketched in figure 2, and not the effective – nor the average – viscosity. We will come back to this point later on. In the remainder of the paper the viscosity perturbation is accounted for, unless otherwise stated.

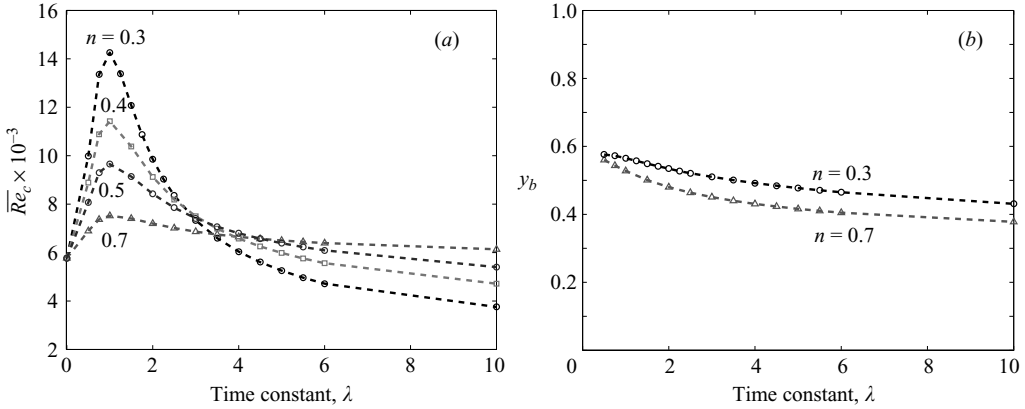


FIGURE 4. Effect of shear thinning on (a) the critical Reynolds number \overline{Re}_c and (b) the position of the reference point y_b where $\mu(y_b) = \bar{\mu}$. The curves are labelled by the flow behaviour index n .

To analyse the effect of shear thinning on the critical conditions, \overline{Re}_c was computed for different values of n and λ . Results are reported in figure 4(a). Note that: (i) at ‘low’ values of the time constant λ , shear thinning stabilizes the flow, and the maximum degree of stabilization is reached for $\lambda \approx 1$, i.e. when the characteristic time associated with the fluid rheology equals the characteristic time of the flow; (ii) for ‘large’ values of λ , shear thinning appears to be destabilizing. This observation agrees with results obtained by Gupta (1999) for the case of power-law fluids, where the Reynolds number is defined with a nominal viscosity, $K(U_c/h)^{n-1}$. We further observe that if the computations are carried out with $\mu' = 0$, only a stabilizing effect is present.

In the discussion so far, the reference viscosity is the average viscosity $\bar{\mu} = \langle \mu \rangle / 2$ of the Carreau fluid. The relevance of this scaling can be assessed by plotting the position y_b where the local effective viscosity $\mu(y_b) = \bar{\mu}$. Figure 4(b) shows that this reference point y_b is away from the wall. Employing an effective viscosity which pertains to a position far from the wall is counterintuitive, since Tollmien–Schlichting waves originate in a near-wall viscous layer. Analysis of the dominant terms of the Orr–Sommerfeld equation in the critical and wall layers helps establish the relevant viscosity scale. In a neighbourhood of $y = y_c$, the Orr–Sommerfeld equation $\mathcal{L}v = \omega \Delta v$, must be rescaled so that viscous terms enter the primary balance. By letting $\hat{v}(\xi) = v(y)$ and $\hat{\mu}_t(\xi) = \mu_t(y)$, with $\xi = (y - y_c)/\epsilon$ and $\epsilon = (\alpha Re dU_b/dy|_{y=y_c})^{-1/3}$, it is simple to see that the critical-layer equation at lowest order reduces to

$$\xi \hat{D}^2 \hat{v} = -i \hat{\mu}_t \hat{D}^4 \hat{v}, \quad (3.2)$$

where $\hat{D} = d/d\xi$. Also, close to the wall at $y = 1$ (and likewise for the lower wall) the boundary layer approximation of the Orr–Sommerfeld equation is

$$D_\chi^2 v^* = -i \mu_t^* D_\chi^4 v^*, \quad (3.3)$$

where $\chi = (y - 1)/\epsilon^*$, $\epsilon^* = (\alpha Re c)^{-1/2}$, $c = \omega/\alpha$, $v^*(\chi) = v(y)$, $\mu_t^*(\chi) = \mu_t(y)$ and $D_\chi = d/d\chi$. It is clear from (3.2) and (3.3) that it is the tangent viscosity that enters the balance in wall and critical layers. This supports the choice of the wall tangent viscosity $\mu_{tw} = \mu_t(y = \pm 1)$ as reference, in place of $\bar{\mu}$.

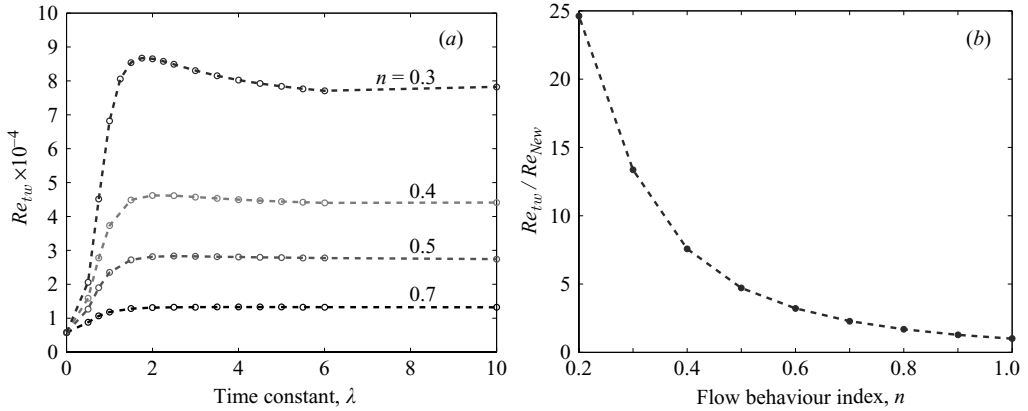


FIGURE 5. Variation of the critical Reynolds number, based on the wall tangent viscosity, (a) with the time constant λ , for different values of n ; (b) asymptotic behaviour for large λ (results obtained by fixing $\lambda = 20$).

When μ_{tw} is adopted in the definition of the Reynolds number,

$$Re_{tw} = \frac{\rho U_c h}{\mu_{tw} \hat{\mu}_0}, \quad (3.4)$$

it is shown in figure 5(a) that shear thinning is consistently stabilizing. Figure 5(b) displays the asymptotic (large- λ) behaviour of Re_{tw} as function of the power-law index n : the critical Reynolds number decreases exponentially with n , and reaches the Newtonian limit when $n = 1$.

In laboratory experiments it is a customary to employ the *effective* viscosity at the wall in the definition of the Reynolds number (see, for instance, Peixinho *et al.* 2005). From measurements of the pressure drop, the wall stress is estimated; rheological diagrams are then used to infer an approximate value of the wall viscosity. If the viscosity perturbation were not taken into account in the equations, the effective wall viscosity would emerge from the critical- and wall-layer equations as the most appropriate reference. Should we adopt the effective viscosity at the wall as scale, to conform to experimental practice, we would find the same qualitative behaviour as with μ_{tw} , as shown by figure 6. However, for the arguments advanced above, we maintain the tangent viscosity at the wall as the most appropriate scale.

To complete the description of the critical conditions, we represent in figure 7(a) the evolution of the streamwise wavenumber with the rheological parameters λ and n . Independently of the flow behaviour index, longer waves are found at criticality when $\lambda \approx 1$; the critical wavenumbers tend to constant values with increasing λ and the asymptotic curve of figure 7(b) displays a non-monotonic behaviour, with shorter waves emerging with the increase of shear thinning for n below 0.6.

Examination of the energy budget provides additional insight into the effect of shear thinning. It is simple to derive the Reynolds–Orr equation for the perturbation energy, by following the procedure that led to (3.1); in symbolic form the equation is

$$\frac{d\langle I_1 \rangle}{dt} = \langle I_2 \rangle - \frac{1}{Re} \langle I_3 \rangle. \quad (3.5)$$

The term on the left-hand side represents the time variation of the disturbance kinetic energy density, $\langle I_2 \rangle$ is the integral of the product of the Reynolds stress with the mean velocity gradient and quantifies the energy available to the perturbation, and $\langle I_3 \rangle / Re$

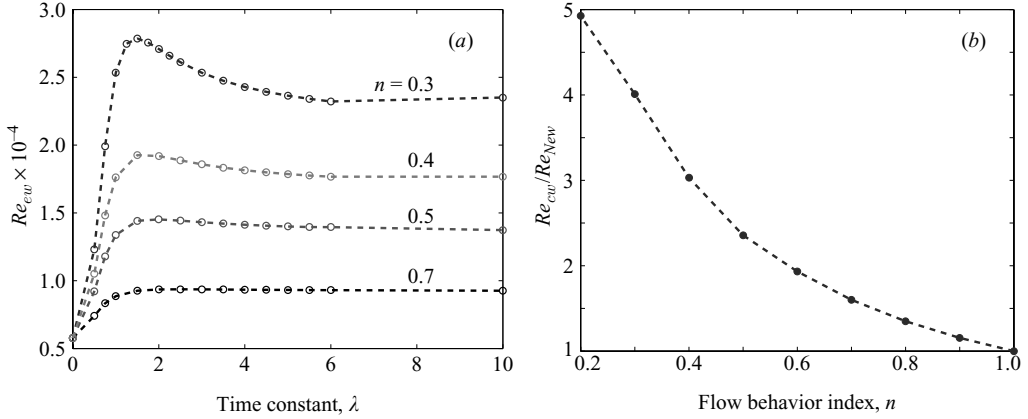


FIGURE 6. As figure 5 but with the critical Reynolds number based on the wall effective viscosity.

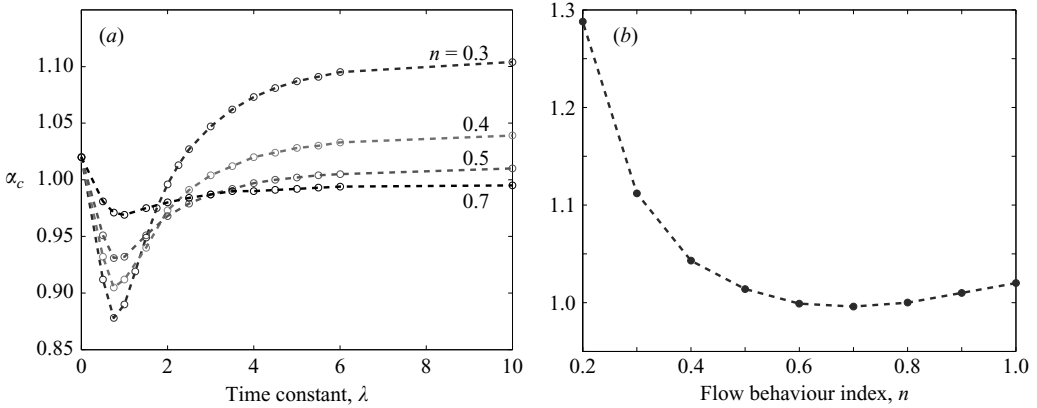


FIGURE 7. Variation of the critical wavenumber with the time constant λ , (a) for different values of n ; (b) asymptotic behaviour for large λ (results obtained by fixing $\lambda = 20$).

is the rate of dissipation of kinetic energy into heat. Following Govindarajan *et al.* (2001), it is convenient to compute and compare the space-averaged production and dissipation terms Γ_{\pm} defined by

$$\Gamma_+ = \frac{\langle I_2 \rangle}{\langle \mathcal{E} \rangle}, \quad \Gamma_- = \frac{1}{Re} \frac{\langle I_3 \rangle}{\langle \mathcal{E} \rangle}, \quad (3.6)$$

with $I_1 = \mathcal{E} \exp(2\omega_1 t)$. At criticality, the transfer of energy from the base flow to the disturbance motion is exactly balanced by viscous dissipation as shown in figure 8 for the case of a Newtonian fluid. The disturbance kinetic energy is supplied mainly in the vicinity of the critical layer, of thickness $O(\alpha Re)^{-1/3}$, while most of the dissipation occurs in the wall layer, which is $O(\alpha Re)^{-1/2}$. The effect of viscosity stratification on the energy budget can be appreciated by comparing the results obtained for a Newtonian fluid (figure 8) with those given in figure 9 for a Carreau fluid. In the latter case we have $Re_{tw} = 5772$, $\lambda = 10$, α corresponds to the critical wavenumber value for the given parameters, and the value of n is either 0.7 or 0.5. With increasing shear

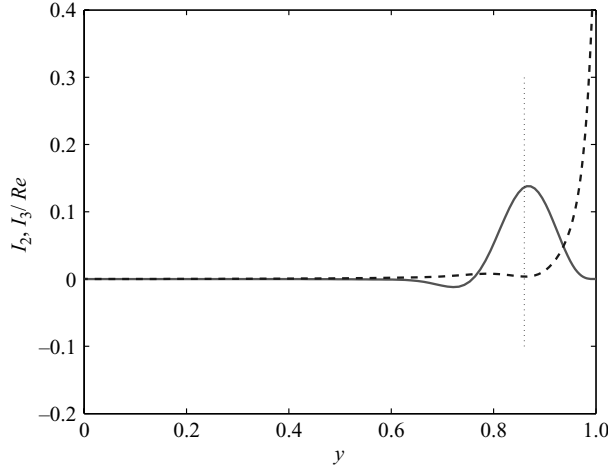


FIGURE 8. Disturbance kinetic energy transfer terms: the production term I_2 is represented by a solid line and the viscous dissipation term I_3/Re is plotted with a dashed line. Newtonian fluid with $Re = 5772$ and $\alpha = 1.02$; $\Gamma_+ = \Gamma_- = 7.394 \times 10^{-3}$. In this figure and the figures to follow the position of the critical layer is shown by a dotted vertical line.

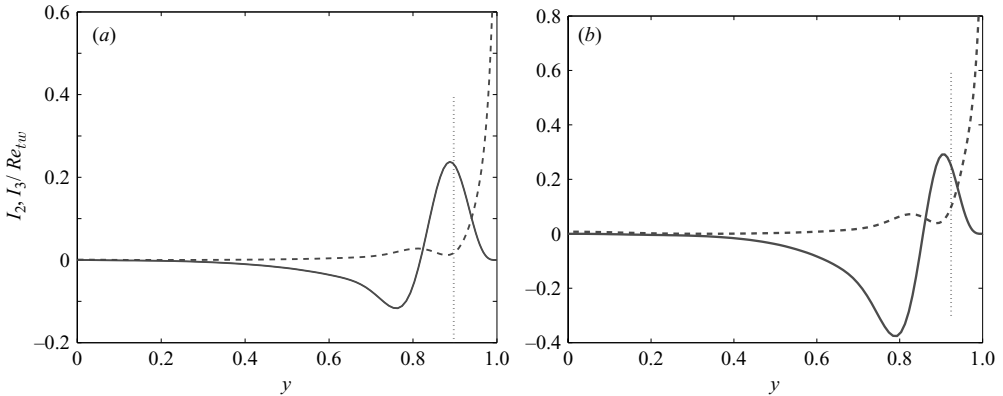


FIGURE 9. Effect of viscosity stratification on the energy budget for a Carreau fluid, $Re_{tw} = 5772$, $\lambda = 10$. (a) $n = 0.7$, $\alpha = 1.12$, $\Gamma_+ = 1.798 \times 10^{-4}$, $\Gamma_- = 9.581 \times 10^{-3}$. (b) $n = 0.5$, $\alpha = 1.264$, $\Gamma_+ = -7.904 \times 10^{-3}$, $\Gamma_- = 1.312 \times 10^{-2}$.

thinning we observe that: (i) the portion of flow domain where the production term I_2 is negative increases, rendering the flow progressively more stable compared to the Newtonian case displayed in figure 8; (ii) the position of the critical point approaches the wall; (iii) the order of magnitude of the average viscous dissipation remains the same as the Newtonian case.

The main factor determining stability or instability of the flow is the exchange of energy between base flow and perturbation, which is driven by the phase change between the two fluctuating velocity components, caused by the viscosity stratification. When the viscosity fluctuation is artificially forced to zero, a large negative production region appears, leading to a fictitious stabilization (see figure 10).

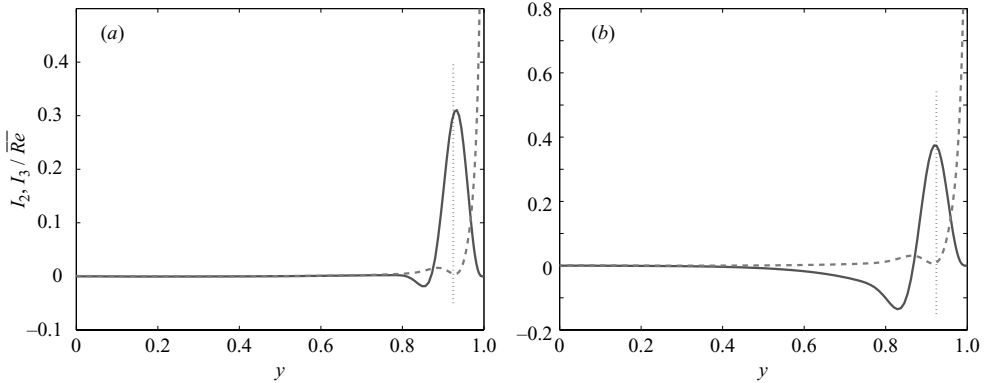


FIGURE 10. Effect of viscosity stratification on the energy budget at $\overline{Re} = 5772$ ($Re_{tw} = 56630$), $n = 0.5$ and $\lambda = 10$. (a) Unstable case with $\alpha = 1.001$, $\Gamma_+ = 6.153 \times 10^{-3}$, $\Gamma_- = 5.700 \times 10^{-3}$. (b) Stable case obtained by artificially imposing $\mu' = 0$, $\alpha = 1.107$, $\Gamma_+ = 1.847 \times 10^{-3}$, $\Gamma_- = 7.769 \times 10^{-3}$.

4. Short-time behaviour: transient growth and optimal disturbances

The transient evolution of perturbations in the linear regime is determined following the methodology described by Schmid & Henningson (1994). For a given Fourier mode, the instantaneous disturbance kinetic energy is given by

$$E_t(\mathbf{q}_0; \alpha, \beta) = \frac{1}{2k^2} \int_{-1}^1 (|\mathbf{D}v|^2 + k^2|v|^2 + |\eta|^2) dy, \quad (4.1)$$

which is function of time and of the initial condition, $\mathbf{q}_0 = (v, \eta)_0^T = \mathbf{q}(y, 0; \alpha, \beta)$. As usual, the gain G is defined as the amplification of the kinetic energy at time t over all non-zero initial conditions:

$$G(t, \alpha, \beta) = \sup_{\mathbf{q}_0 \neq 0} \left(\frac{E_t(\mathbf{q}_0, \alpha, \beta)}{E_0(\mathbf{q}_0, \alpha, \beta)} \right); \quad (4.2)$$

then the maximum transient energy growth possible over all times is $G_{max}(\alpha, \beta) = \sup_{t \geq 0} G(t, \alpha, \beta)$. The maximum of G_{max} for all the pairs (α, β) is denoted G^{opt} which is reached by the optimal perturbation at a specific time t^{opt} . Unlike the exponential amplification case, here the growth of disturbances occurs over a relatively short initial time and is related to an inviscid mechanism, the *lift-up* of low-speed streaks from the wall. Viscosity acts only to moderate the amplification and also, in this case, employing a wall-based viscosity appears reasonable.

We have initially employed $\bar{\mu}$ to compare with the results obtained by Chikkadi *et al.* (2005), and have thus used the following parameters: $\overline{Re} = 1000$, $n = 0.5$ and $\lambda = 2$. In figure 11(a), the curve labelled (2) is in very good agreement with that given by Chikkadi *et al.* (2005) (see their figure 4); the curve labelled (1), which accounts for μ' , displays an amplification which is up to 27% larger and G^{opt} reaches 230 at a time of 81. It is thus clear that the conclusion by Chikkadi *et al.* (2005) that transient behaviour is unaffected by stratification of viscosity must be revised. The apparent enhanced growth experienced by a shear-thinning fluid compared with a Newtonian fluid occurs in the presence of a ‘fuller’ base velocity profile and this is at odds with previous transient growth studies (Corbett & Bottaro 2000; Fransson & Corbett 2003). Figure 11(b) helps reconcile physical intuition with numerical results:

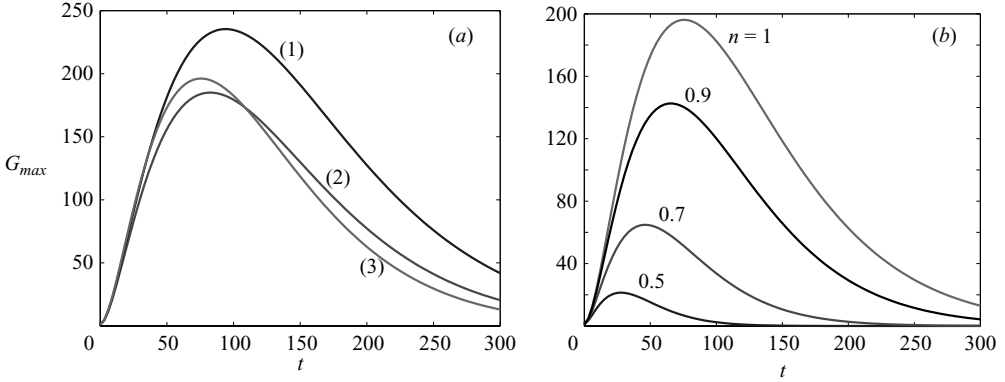


FIGURE 11. Energy amplification at $\lambda=2$, $\alpha=0$, $\beta=2.05$. (a) $\overline{Re}=1000$ and $n=0.5$. For the curve labelled with (1) μ' is taken into account; for curve (2) μ' is forced to zero; curve (3) pertains to a Newtonian fluid. (b) $Re_{tw}=1000$ and different values of n .

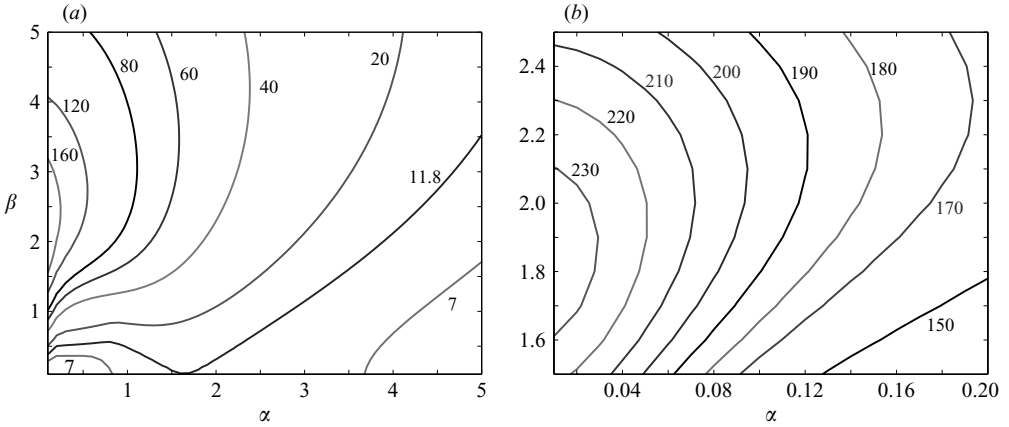


FIGURE 12. Isolines of maximum gain $G_{max}(\alpha, \beta)$ for $Re_{tw}=4584$ at $n=0.5$ and $\lambda=2$. (b) A close-up in the low- α region in (a).

the amplification factor G at $Re_{tw}=1000$, $\alpha=0$, $\beta=2.05$, $\lambda=2$, is shown for different values of the shear-thinning index n . The case $n=1$ coincides with the Newtonian case for $Re=1000$, i.e. $G^{opt}=196$ at $t^{opt}=75.9$ (Schmid & Henningson 2001). The effect of shear thinning is to reduce significantly the maximum growth attainable at fixed Re_{tw} , and the corresponding time, by the approximate scalings

$$\frac{G_{n \neq 1}^{opt}}{G_{n=1}^{opt}} \approx n^{3.60}, \quad \frac{t_{n \neq 1}^{opt}}{t_{n=1}^{opt}} \approx n^{1.57},$$

which apply when λ is large enough. A similar stabilizing effect of shear thinning would have arisen had we used a Reynolds number based on the effective wall viscosity. The optimal horizontal scales of motion do not differ much from the Newtonian case.

To obtain a complete picture of the transient growth dependence on the horizontal wave vector, the maximum growth is calculated for a range of wavenumbers and plotted in the (α, β) -plane. An example of contours of G_{max} for $Re_{tw}=4584$ ($\overline{Re}=1000$) at $n=0.5$ and $\lambda=2$ is provided in figure 12. The optimal perturbation occurs at $\alpha=0$ and $\beta=1.93$, and $G^{opt}=236.8$ is reached after $t^{opt}=99$ advective time

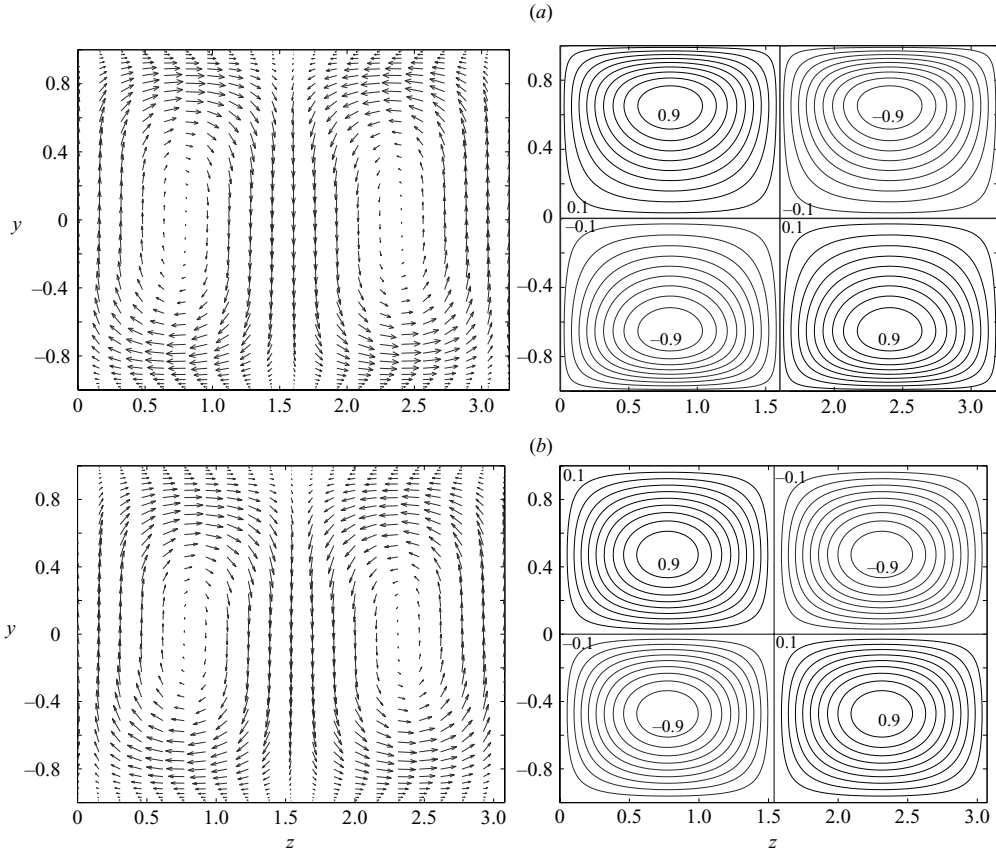


FIGURE 13. Optimal perturbation and optimal streaks for (a) Carreau fluid at $Re_{tw} = 4584$ ($\overline{Re} = 1000$), $n = 0.5$, $\lambda = 2$ and (b) Newtonian fluid at $Re = 1000$. On the left the velocity vectors $ve_y + we_z$ of the optimal perturbation at $t = 0$ are plotted; on the right equally spaced contours of the streamwise velocity u at $t = t^{opt}$ are displayed.

units. The numerical results show that around these optimal conditions the transient behaviour is weakly dependent on β whereas the variation with the streamwise wavenumber is rather rapid. For comparison, in the Newtonian case at $Re = 4584$ the optimal disturbance is found at $\alpha = 0$, $\beta = 2.04$, and after $t^{opt} = 348$ the amplification reaches $G^{opt} = 4119$ (Biau & Bottaro 2004). In the range $0.2 \leq n \leq 1$ and $0 \leq \lambda \leq 10$, it is found that the optimal perturbation is formed by streamwise vortices ($\alpha = 0$) with longer spanwise wavelength when the shear-thinning character becomes more important, i.e. when the viscosity contrast between the axis and the wall is stronger.

The velocity field $ve_y + we_z$ associated with the optimal perturbation is displayed in figure 13. It is characterized by two counter-vortices which transform into streaks at $t = t^{opt}$. In this respect the ‘optimal’ behaviour is analogous to that of Newtonian fluids. Nevertheless, for shear-thinning fluids, the maximum in the longitudinal speed of the streak approaches the walls where the effective viscosity is lower.

A global view of the effect of shear thinning on the optimal transient amplification of disturbances is provided in figure 14. In figure 14(a), the Reynolds number is based on the viscosity averaged across y , and in figure 14(b) it is based on μ_{tw} . Figure 14(a) appears to demonstrate that shear thinning significantly enhances the

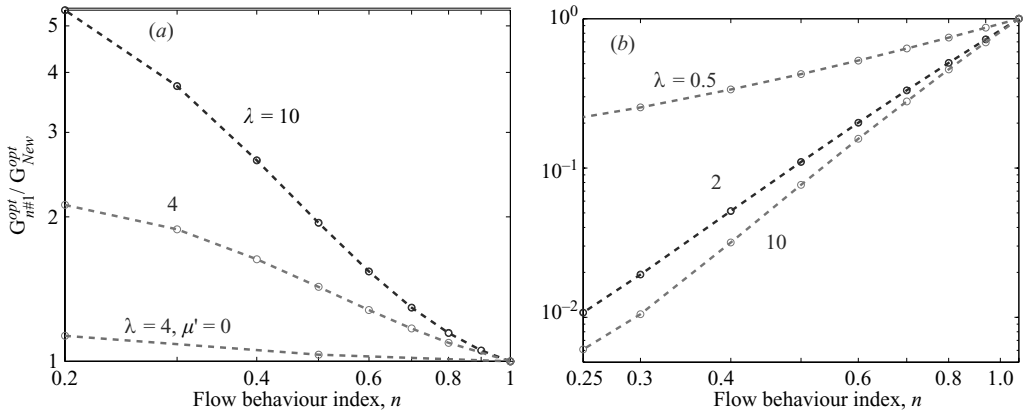


FIGURE 14. Effect of the shear thinning on the optimal amplification: (a) $\overline{Re} = 1000$, (b) $Re_{tw} = 1000$.

amplification experienced by ‘optimal’ initial streaks compared to the Newtonian case (with a negligible effect for the case in which μ' is neglected). Exactly the opposite effect is found by using as scale the tangent viscosity at the wall (figure 14b). As in the case of the exponential growth, the curves collapse onto one another for λ sufficiently large.

5. Conclusions

The linear stability of viscously stratified channel flow (with the viscosity modelled by the Carreau law) has been revisited, focusing on both exponentially and algebraically growing perturbations. The motivation for this study comes from the possibility of delaying transition to turbulence by creating a viscosity contrast in the channel. We have accounted for a non-vanishing viscosity disturbance μ' , and this yields an anisotropic disturbance stress tensor.

The results we arrive at contradict previously reported conclusions. Part of the disagreement stems from the neglect of μ' in past studies, and part arises from the choice of the viscosity used to define the Reynolds number. Whereas in the past it has been deemed appropriate to use the average effective viscosity to produce results for shear-thinning fluids (to compare with corresponding results for the Newtonian case), we argue here that the tangent viscosity evaluated at the wall is a more pertinent choice. Although the selection of the viscosity scale appears to be simply a matter of choice, the conclusions from comparing different shear-thinning fluids among themselves and to Newtonian fluids can be radically different depending on that choice.

For the case of two-dimensional exponentially growing waves the choice of the wall tangent viscosity as the relevant scale is dictated by the asymptotic behaviour of the flow in the wall and critical layers. It is found that the instability occurs much earlier than previously reported for a range of material time constants λ and power-law indices n , as a consequence of the more efficient transfer of disturbance energy across the critical layer compared to the $\mu' = 0$ case. The largest stabilization occurs for $\lambda \approx 1.5$ (independent of n) and the stabilizing effect is maintained for arbitrarily large values of λ .

For the transient growth of three-dimensional waves in the subcritical regime, previous results indicated that shear thinning had negligible influence. Our main conclusion is embodied by figure 14: whilst shear thinning appears to be destabilizing when Re is based on the average effective viscosity, the opposite effect appears when the (tangent or effective) viscosity at the wall is used. The superiority of a wall-based viscosity in describing the physics of the problem cannot be easily ascertained on asymptotic grounds. However, the lift-up effect is an inviscid phenomenon and viscosity acts primarily in a near-wall layer to moderate the growth of streaks: thus, it seems reasonable to employ a wall-based viscosity to describe this diffusive effect. Choosing $\bar{\mu}$ underestimates the effective Reynolds number.

In all situations considered here it has been found that the transition is effectively postponed when a viscosity contrast is produced in the critical layer. Although the results were presented only for the case of Carreau fluids, we expect that the conclusions reported in this paper are qualitatively unaffected when another shear-thinning model is used. This is supported by unpublished results obtained by our group for power-law fluids. Current work focuses on the viscosity contrast needed to optimally delay transition to turbulence.

A. B. acknowledges the support and the hospitality he benefitted from at LEMTA while carrying out part of this work. We thank Professor Rama Govindarajan for useful comments on the manuscript and for providing the unpublished data points plotted in figure 2.

REFERENCES

- BIAU, D. & BOTTARO, A. 2004 Optimal perturbations and minimal defects: Initial paths of transition to turbulence in plane shear flows. *Phys. Fluids* **16**, 3515.
- BIRD, R. B., ARMSTRONG, R. & HASSAGER, O. 1987 *Dynamics of polymeric liquids*. Wiley-Interscience.
- CARREAU, P. J. 1972 Rheological equations from molecular network theories. *Trans. Soc. Rheolo.* **16**, 1, 99.
- CHARRU, F. & HINCH, E. J. 2000 “Phase diagram” of interfacial instabilities in a two-layer Couette flow and mechanism of the long-wave instability. *J. Fluid Mech.* **414**, 195.
- CHIKKADI, V., SAMEEN, A. & GOVINDARAJAN, R. 2005 Preventing transition to turbulence: A viscosity stratification does not always help. *Phys. Rev. Lett.* **95**, 264504.
- CORBETT, P. & BOTTARO, A. 2000 Optimal perturbations for boundary layers subject to stream-wise pressure gradient. *Phys. Fluids* **12**, 120.
- CRAIK, A. D. D. 1969 The stability of plane Couette flow with viscosity stratification. *J. Fluid Mech.* **36**, 685.
- DE ANGELIS, E., CASCIOLA, C. M. & PIVA, R. 2002 DNS of wall turbulence: dilute polymers and self-sustaining mechanisms. *Comput. Fluids* **31**, 495.
- DRAZIN, P. G. & REID, W. H. 1981 *Hydrodynamic Stability*. Cambridge University Press.
- ERN, P., CHARRU, F. & LUCHINI, P. 2003 Stability analysis of a shear flow with strongly stratified viscosity. *J. Fluid Mech.* **496**, 295.
- FARRELL, B. F. & IOANNOU, P. J. 1998 Perturbation structure and spectra in turbulent channel flow. *Theor. Comput. Fluid Dyn.* **11**, 237.
- FRANSSON, J. H. M. & CORBETT, P. 2003 Optimal linear growth in the asymptotic suction boundary layer. *Eur. J. Mech. B Fluids* **22**, 259.
- GAD-EL-HAK, M. 2000 *Flow Control: Passive, Active, and Reactive Flow Management*. Cambridge University Press.
- GOVINDARAJAN, R. 2002 Surprising effects of minor viscosity gradients. *J. Indian Inst. Sci.* **82**, 121.
- GOVINDARAJAN, R., L'VOV, V. S. & PROCACCIA, I. 2001 Retardation of the onset of turbulence by minor viscosity contrasts. *Phys. Rev. Lett.* **87**, 174501.

- GOVINDARAJAN, R., L'VOV, V. S., PROCACCIA, I. & SAMEEN, A. 2003 Stabilization of hydrodynamic flows by small viscosity variations. *Phys. Rev. E* **67**, 026310.
- GUPTA, G. K. 1999 Hydrodynamic stability of the plane Poiseuille flow of an electro-rheological fluid. *Intl J. Non Linear Mech.* **34**, 589.
- HINCH, E. J. 1984 A note on the mechanism of the instability at the interface between two viscous fluids. *J. Fluid Mech.* **144**, 463.
- HOOPER, A. & BOYD, W. 1983 Shear-flow instability at the interface between two viscous fluids. *J. Fluid Mech.* **128**, 507.
- LI, W., XI, L. & GRAHAM, M., D. 2006 Nonlinear travelling waves as a framework for understanding turbulent drag reduction. *J. Fluid Mech.* **565**, 353.
- LUMLEY, J. L. 1969 Drag reduction by additives. *Annu. Rev. Fluid Mech.* **1**, 367.
- MALIK, S. V. & HOOPER, A. P. 2005 Linear stability and energy growth of viscosity stratified flows. *Phys. Fluids* **17**, 024101.
- METZNER, A. B. 1977 Polymer solution and fiber suspension rheology and their relationship to turbulent drag reduction. *Phys. Fluids* **20**, S145.
- NOUAR, C., KABOUYA, N., DUSEK, K. & MAMOU, M. 2007 Modal and non-modal linear stability of the plane-Bingham-Poiseuille flow. *J. Fluid Mech.* **577**, 211.
- ORLANDI, P. 1997 A tentative approach to the direct simulation of drag reduction by polymers. *J. Non-Newtonian Fluid Mech.* **60**, 277.
- PEIXINHO, J., NOUAR, C., DESAUBRY, C. & THÉRON, B. 2005 Laminar transitional and turbulent flow of yield stress fluid in a pipe. *J. Non-Newtonian Fluid Mech.* **128**, 175.
- PINARBASI, A. & LIAKOPOULOS, A. 1995 The role of variable viscosity in the stability of channel flow. *Intl Commun. Heat Mass Transfer* **22**, 837.
- PINARBASI, A. & OZALP, C. 2001 Effect of viscosity models on the stability of a Non-Newtonian fluid in a channel with heat transfer. *Intl Commun. Heat Mass Transfer* **28**, 369.
- RANGANATHAN, B. T. & GOVINDARAJAN, R. 2001 Stabilization and destabilization of channel flow by location of viscosity-stratified fluid layer. *Phys. Fluids* **13**, 1.
- SAMEEN, A. & GOVINDARAJAN, R. 2007 The effect of wall heating on instability of channel flow. *J. Fluid Mech.* **577**, 417.
- SCHMID, P. J. & HENNINGSON, D. S. 1994 Optimal energy density growth in Hagen-Poiseuille flow. *J. Fluid Mech.* **277**, 197.
- SCHMID, P. J. & HENNINGSON, D. S. 2001 *Stability and Transition in Shear Flows*. Springer.
- STONE, P. A., ROY, A., LARSON, R., WALEFFE, F. & GRAHAM, M. D. 2004 Polymer drag reduction in exact coherent structures of plane shear flow. *Phys. Fluids* **16**, 3470.
- SURESHKUMAR, R., BERIS, A. N. & HANDLER, R. A. 1997 Direct numerical simulation of the turbulent channel flow of a polymer solution. *Phys. Fluids* **9**, 743.
- TANNER, R. 2000 *Engineering Rheology*. Oxford University Press.
- TREFETHEN, L. N., TREFETHEN, A. E., REDDY, S. C. & DRISCOLL, T. A. 1993 Hydrodynamic stability without eigenvalues. *Science* **261**, 578.
- WALL, D. P. & WILSON, S. K. 1996 The linear stability of channel flow of fluid with temperature-dependent viscosity. *J. Fluid Mech.* **323**, 107.
- YIH, C.-S. 1967 Instability due to viscosity stratification. *J. Fluid Mech.* **27**, 337.
- ZHANG, K., ACRIVOS, A. & SCHAFLINGER, U. 1992 Stability in a two-dimensional Hagen-Poiseuille resuspension flow. *Intl J. Multiphase Flow* **18**, 51.